Extension of the Air Distribution Network Design Optimization algorithm: implementation of fittings

Sandy Jorens [a], *Zakarya* Kabbara [a], Ehsan Ahmadian[a], *Ivan* Verhaert [a]

[a] Research Group BEASt (Built Environment Assessing Sustainability), Faculty of Applied Engineering: Electromechanics, University of Antwerp, Antwerp, Belgium, sandy.jorens@uantwerpen.be.

Abstract. The number of requirements that heating, ventilation, and air conditioning (HVAC) systems in buildings have to fulfill continues to rise. Design engineers are being challenged to design HVAC systems with high standards of performance considering, comfort and energy efficiency. These conflicting objectives have to be achieved within a limited budget and time. Presently, considerable reliance is still placed on rules of thumb and the designer's experience, which often results in sub-optimal designs. More than ever, there is a need for practically usable design tools. Especially in the field of centralized air distribution system design, user-friendly tools are needed to support the design engineer. In previous research, an air distribution network design (ADND) optimization algorithm was developed. The ADND algorithm is a heuristic optimization algorithm that automatically generates numerous different air distribution system configurations (i.e., ductwork layout and sizing) for non-residential buildings while minimizing the material costs. Although the ADND algorithm shows promising results, some additions are still required before the algorithm can be used in practice. Currently, the objective function is limited to the minimization of material costs. However, other objectives, e.g., minimization of energy costs or noise levels, are not yet considered. Moreover, the generated configurations are based on the aeraulic performance of only circular and rectangular ducts. Fittings and other ventilation components (e.g. silencers and diffusers) are not yet included. In this research, the ADND optimization algorithm was improved by implementing fittings (i.e., bends, reducers, tees, and cross fittings) in the optimization algorithm. A practical test case demonstrates the extended ADND optimization algorithm.

Keywords. Air distribution system design, layout optimization, fittings, zeta values, heuristics, test case.
DOI: https://doi.org/10.34641/clima.2022.99

1. Introduction

1.1 Design of centralized air distribution systems

Nowadays, design engineers are being challenged to design HVAC systems with high standards of performance considering, comfort, and energy efficiency, while time and budget are limited. To achieve these (conflicting) objectives, the design engineer is left with numerous difficult decisions.

When designing centralized air distribution systems in non-residential buildings, a major part of these decisions is related to the air distribution system's configuration, i.e., the ductwork layout and duct and fan sizing. The complexity of this design problem is determined not only by its conflicting objectives, but also by numerous linear and non-linear constraints to which the decisions are subjected (e.g., limitations on space, duct sizes, and fan pressure)[1]. Therefore, a simulation-based tool for informed decision-making could benefit design engineers to achieve superior ventilation systems with optimal performance.

Although both the ductwork layout and ducts and fan sizing, have a significant impact on the performance and the total cost of the air distribution system, most design methods are limited to the ducts and fan sizing [2-5]. The layout itself is predetermined using rules of thumb and the designer's experience, which results in workable designs, but not necessarily optimal designs. Even when, for example, drawing tools are used that partly automate the drawing of the layout, a comparison of different layouts in terms of costs and other performance parameters is still lacking.

To overcome this shortcoming, Jorens et. al. (2018)

Copyright ©2022 by the authors. This conference paper is published under a CC-BY-4.0 license.

introduced a novel optimization problem, i.e., the air distribution network design (ADND) optimization problem [1]. In this problem, the optimal ductwork layout is determined jointly with the duct and fan sizes, while minimizing the total cost of the system. The authors also laid the basic strategy to solve this novel optimization problem by developing a novel heuristic algorithm, i.e., the ADND algorithm [6]. The ADND optimization algorithm can generate different air distribution system configurations for buildings with varying characteristics while minimizing material costs.

1.2 ADND algorithm

The ADND algorithm starts from a building's floor plan where all demand nodes (= diffusers) with the corresponding design airflow rates are indicated, as well as all the potential duct and fan locations.

Graph theory [7] is used to represent this floor plan as a rooted undirected weighted graph G(N, E), with E being the set of edges representing potential air ducts and N the set of nodes or vertices representing potential supply nodes (fans), demand nodes (terminal units or diffusers), and junctions (fittings). Additionally, several constraints are specified and given as input to the ADND algorithm, e.g., maximum duct heights, maximum air velocities, and maximum fan pressure. These constraints depend on local standards, the customer's preferences, and the building's restrictions. For example, when the ductwork has to run above a suspended ceiling, the available building space is limited, which impacts the maximum allowable duct height. Figure 4 and appendix 1 give an example of the algorithm's input data (see section 3 Test case).

The ADND algorithm consists of two major phases, i.e., a construction phase and a local search phase. In the first phase, complete air distribution system configurations are generated from scratch and evaluated for feasibility. A feasible layout can be seen as a directed tree, without loops, that connects the root node (i.e., fan) to all demand nodes (i.e., diffusers) in the graph (e.g., figure 5 gives an example of a feasible layout). To generate numerous feasible layouts, an adapted randomized version of Prim's algorithm is applied [6,7]. Adapted in the sense that a layout generation starts from a predefined root node instead of a random node and that the ending solution does not need to be a spanning tree. The stopping criterion is achieved when all demand nodes are part of the tree. Instead of growing the tree by adding the edge with minimal weight each time, this edge is chosen randomly to increase the variety of the generated layouts. After generating the layouts, the ADND algorithm continues with an initial sizing of the ductwork using average velocities [5]. All resulting configurations are subjected to a feasibility check to evaluate if each configuration meets the predefined constraints (e.g., maximum duct height constraints [6]). The second phase of the ADND algorithm, i.e., the local search phase, optimizes the duct sizes of every feasible layout in terms of material costs. A steepest descent-mildest ascent strategy is chosen as a move strategy. This means that every move results in the best possible improvement or the least possible deterioration. Specific for the ADND optimization problem, duct sizes are decreased one by one (starting with the biggest ducts first) until a predefined maximum pressure constraint is exceeded. Next, duct sizes are increased again one by one (starting with the smallest ducts first), until the maximum pressure constraint is satisfied again.

The result of the ADND algorithm is a list of feasible ADN configurations, sorted by material price. Although the objective function is defined as a single objective function, the ADND optimization algorithm does allow the user to make a tradeoff between the material costs and energy use. For every feasible configuration that is generated, the following data is calculated: ductwork costs, pressure loss in every path of the network, theoretical fan power, and the pressure difference between the critical path and the path with the lowest pressure loss.

1.3 ADND algorithm: shortcomings

Before the algorithm can be used in practice, some features still need to be added. Besides the ductwork, other ventilation components still have to be integrated into the algorithm, e.g., fittings, silencers, filters, diffusers, and dampers. Moreover, the objective function should include not only the material costs but also other costs, such as maintenance, installation, and energy costs.

In this paper, the ADND algorithm is extended by implementing both circular and rectangular fittings in the algorithm. Specifically, the following fittings were integrated: bends, tees, cross fittings, and reducers. Section 2, first discusses which models are used to calculate the pressure losses of all fittings. Secondly, we discuss how the ADND algorithm automatically detects all fittings (location and type) in an ADN configuration.

2. Fittings

2.1 Fittings modeling

The pressure drop due to a bend or reducer is calculated with the following equation:

$$\Delta p = \xi * \frac{\rho * v^2}{2} \tag{1}$$

Where:

- Δp = pressure drop (Pa),
- ξ = local loss coefficient (/),
- ρ = density (kg/m^3),
- v = velocity (m/s).

The pressure drops due to tees and cross fittings (figure 1) are calculated with equations 2 and 3.

$$\Delta p = \xi_{c,s} * \frac{\rho * v_c^2}{2} \quad (2)$$

and

$$\Delta p = \xi_{c,b} * \frac{\rho * v_c^2}{2} \quad (3)$$

Where:

- $\xi_{c,s}$ = loss coefficient straight path S (/)
- $\xi_{c,b}$ = loss coefficient branch path B (/)
- v_c = air velocity in the common duct C (m/s).

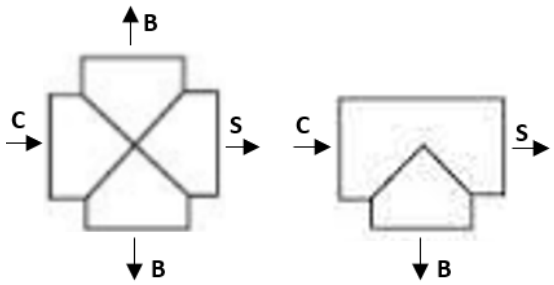

Fig. 1 – A cross (left) and a tee (right)

Depending on the fitting type, the local loss coefficient ξ depends on different parameters (e.g., cross-sectional area or the ratio of inlet area over the outlet area). The required ξ value can be looked up in tables. In this research, the duct fitting database of ASHRAE [2] was implemented in the ADND algorithm to calculate the local loss coefficients. Appendix 2 gives an overview of the different fitting types that are implemented in the ADND algorithm. It should be noted that the algorithm applies linear interpolation when the input values of the models are between index values of the rows and columns of the ASHRAE tables.

2.2 Automatic fitting detection

The detection of the fittings takes place at the end of the construction phase, i.e., after the initial sizing of the feasible layouts. The flowchart in figure 2 gives an overview of the different steps that the algorithm has to go through to determine all junction types of an air distribution network layout.

To clarify the detection process, a simplified example is used. Assume that figure 3 represents a feasible layout that consists of four ducts: [0,1], [1,2], [1,3] and [2,4]. Node 0 is the fan, nodes 3 and 4 are demand nodes, and nodes 1 and 2 are junctions.

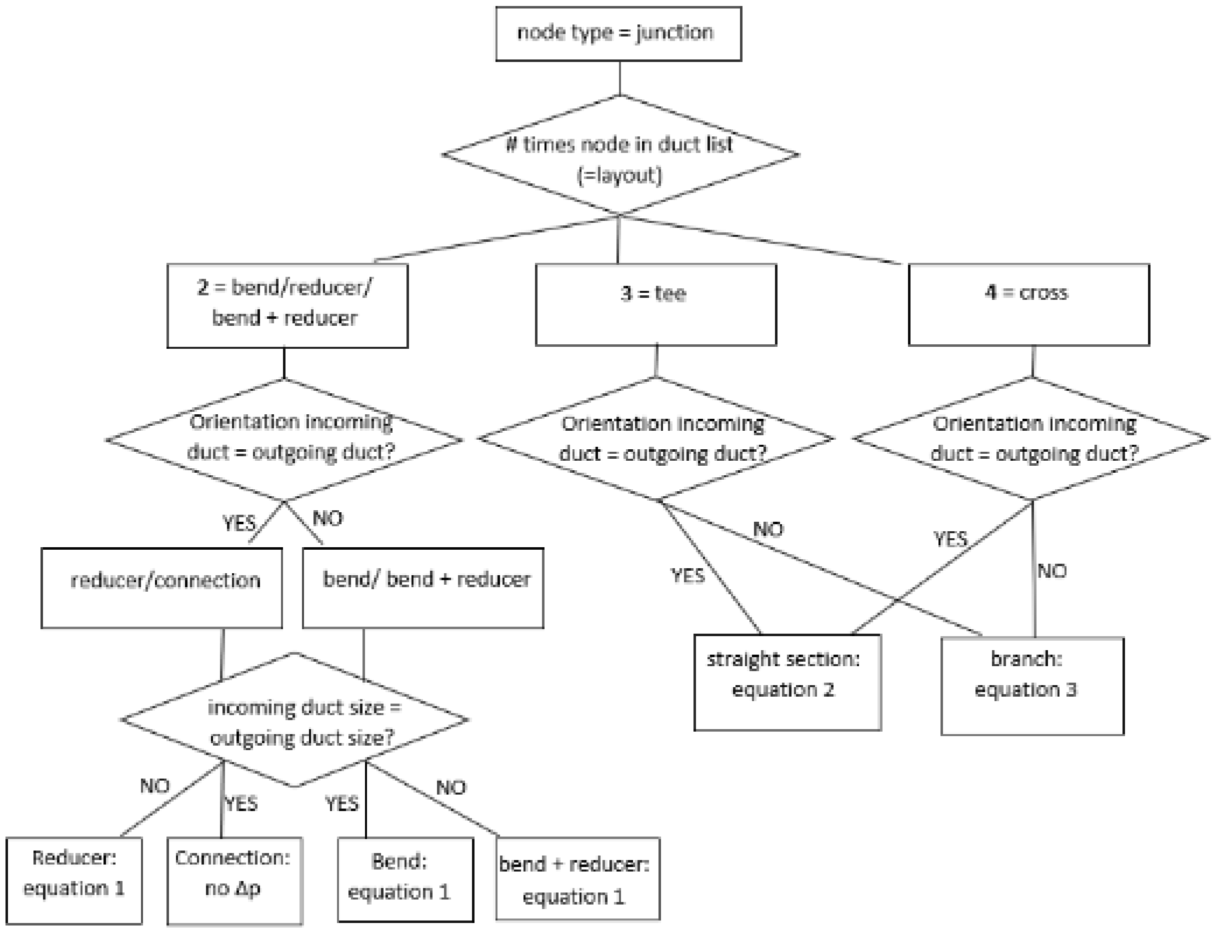

Fig. 2 – Flow chart: automatic fitting detection

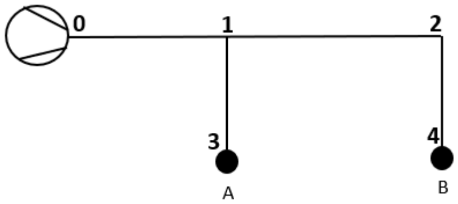

Fig. 3 – A simple air distribution network

According to the flowchart (figure 2), the first step is to count the number of times a junction occurs in the duct list. In this case, there are 2 junctions, i.e., node 1 and node 2. Node 2 occurs two times in the duct list (i.e., one time as an end node in duct [1,2] and one time as a start node in duct [2,4]). This means that node 2 is either a bend, a combination of a bend and a reducer, or a reducer. Next, the algorithm determines if both the incoming [1,2] and outgoing ducts [2,4] have the same or different orientations to specify the node type. For the algorithm to be able to identify a duct orientation (i.e. straight or branch), coordinates have to be first introduced. Until now, a node was characterized solely by a node name and a type. Now, coordinates are added as additional parameters for every node. This means that every node is not only characterized by its name and type, but also by an x and y coordinate. To compare the orientation of two adjacent ducts, the x and y coordinates of the first duct's start node are compared with the x and y coordinates of the second duct's end node. If both coordinates are different, the orientation of the ducts is not the same. If either the x coordinates or the y coordinates are equal, the ducts have the same orientation (i.e., straight).

In the example layout, duct [1,2] has a different orientation than duct [2,4]. Consequently, node 2 is a bend or a combination of a bend and a reducer. If the dimensions of the incoming and outgoing duct are equal, node 2 can be defined as a bend. If not, node 2 is a combination of a bend and a reducer. Similar to this example, the ADND algorithm can identify the other fitting types as well.

3. Test Case

In this section, a simplified, but realistic test case demonstrates some of the capabilities of the extended ADND algorithm.

3.1 Input data

Figure 4 shows one floor of a small office building. The location of all demand nodes and the associated airflow rates (in m^3/h) are indicated on the floor plan (x), as well as all potential duct locations (black lines) and potential junctions (black dots). In total, there are 37 nodes, i.e., one root node (i.e., fan), 13 demand nodes, and 23 junctions. The fan is located in the technical room on the top floor of the building. An overview of the input data for the ducts can be found in appendix 1 as well. All potential ducts that can be installed in the building are listed, where each duct is characterized by a start and end node (i.e., red numbers in figure 4), and a length. Additionally, all ducts must comply with the maximum height and velocity restrictions that have been set (i.e., H_{max} and v_{max}).

3.2 Results

In this paper, two scenarios are simulated. In the first case, the maximum pressure constraint of the critical path is set at 30 Pa, and in the second case at 50 Pa. The best (i.e., cheapest) resulting configurations are displayed graphically in figure 5. Additionally, table 1 compares the two solutions in terms of several evaluation parameters.

As can be seen, the ADND algorithm calculates the total volumetric flow rate (m^3/h), ductwork costs (€), the total pressure loss of the critical path (Pa), and the theoretical fan power (W) for every solution. Since a direct relation exists between the fan power and the energy use, this evaluation parameter gives more insight into the energy use of a solution. Last, the ADND algorithm calculates the pressure difference between the critical path and the path of minimum pressure loss (Pa). According to the pressure balancing constraint, this parameter should be as low as possible [6].

Tab. 1 – Test case results

	Solution 1 (max 30Pa)	**Solution 2 (max 50 Pa)**
Flow rate (m^3/h)	3420	3420
Duct costs (€)	1220	1179
Δp critical (Pa)	29.96	49.56
Theoretical fan power (W)	28.46	47.08
$\Delta p_{max} - \Delta p_{min}$ (Pa)	13.05	34.17

It should be noted that the following assumptions were made for the pressure and price calculations.

- Constant air density (1.2 kg/m^3).
- Ductwork material: galvanized steel (roughness e = $0.15*10^{-3}$ m).
- Fully developed airflow in all ducts and fittings.
- The total pressure loss of the critical path includes the pressure losses of both the ductwork and the fittings. The material cost, however, solely includes the ductwork costs and is based on the price list of manufacturer Lindab [8].

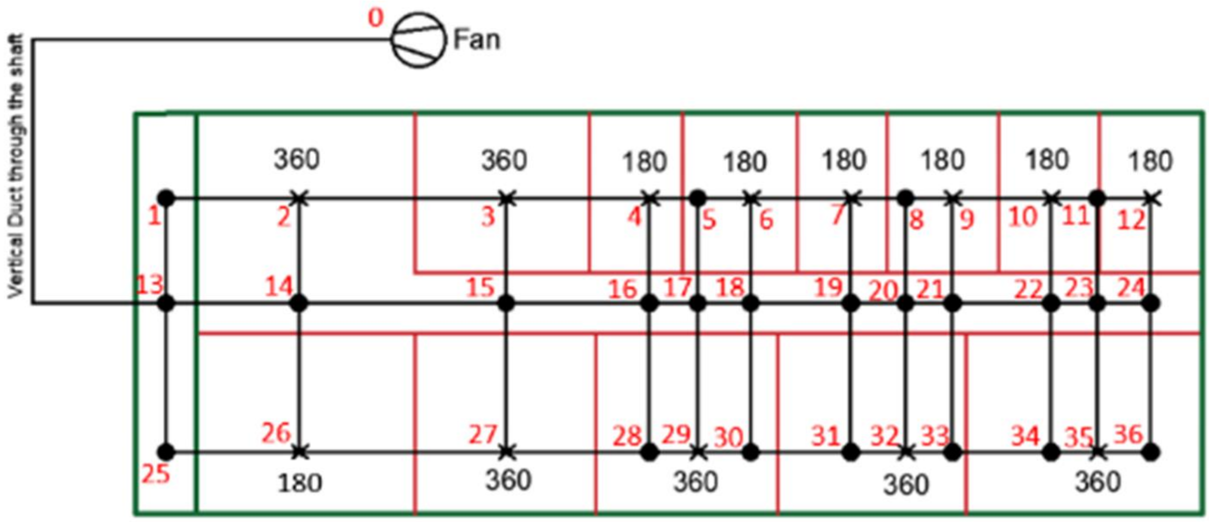

Fig. 4 – Floor plan of one floor in an office building (= input graph ADND algorithm), where all demand nodes with corresponding flow rates in m³/h (x), root node (fan), potential ducts (black lines), and potential junctions (black dots) are indicated

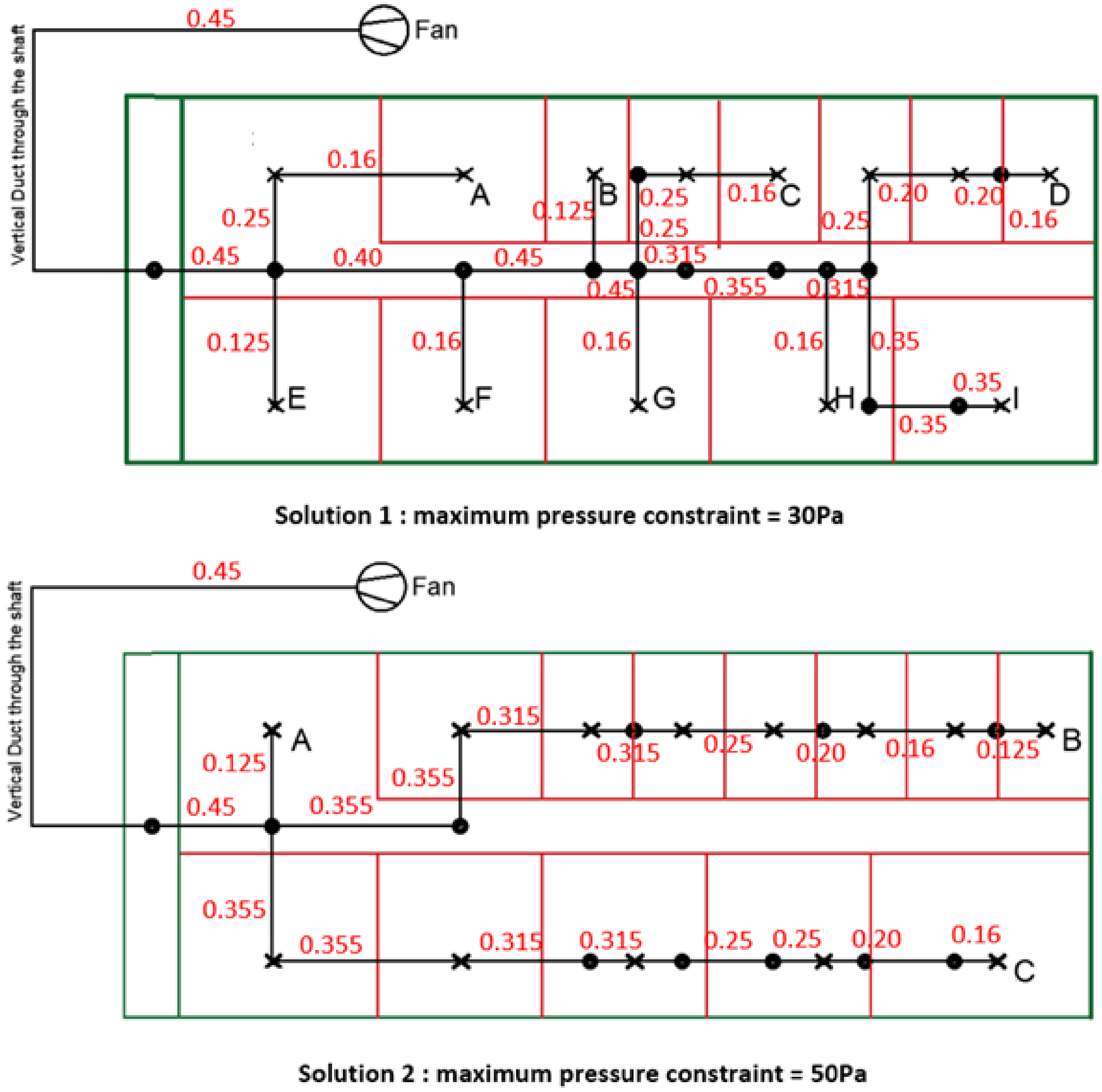

Fig. 5 – The two best resulting ADN configurations, generated with the ADND algorithm (duct dimensions in m)

3.3 Discussion

As can be observed in table 1, there is a relatively small price difference between solutions 1 and 2. Solution 2 is 3.4% cheaper than solution 1. The difference in fan power, however, is very significant. The fan power of solution 2 is not less than 65% higher than the fan power of solution 1.

This can be explained using the graphs presented in figures 6 and 7. Figure 6 presents the pressure drop (Pa) in a duct as a function of the air velocity (m/s). The pressure loss in a duct grows exponentially with increasing air velocity. Figure 7, on the other hand, shows the relation between the pressure loss in the branch part of a tee (Pa) and the inlet air velocity (m/s). As can be observed, the pressure loss rises substantially once the air velocity exceeds 4 m/s.

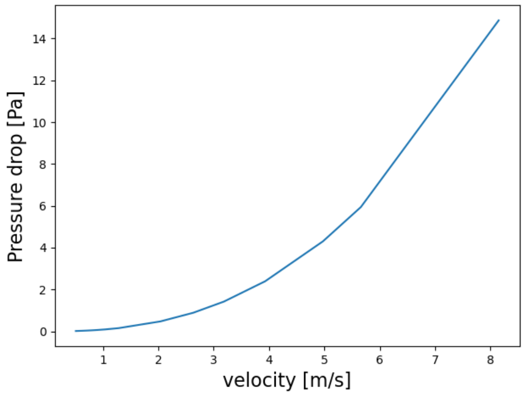

Fig. 6 – Pressure drop (Pa) in a 2m galvanized steel duct vs the velocity (m/s)

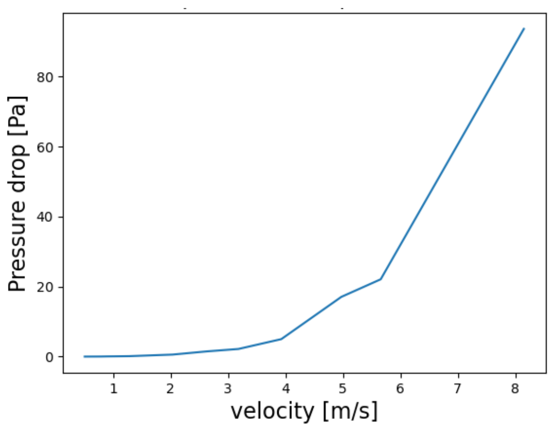

Fig. 7 – Pressure drop (Pa) in the branch part of a circular tee vs velocity (m/s) in the common duct

The pressure drop constraint of 30 Pa (i.e., solution 1) has resulted in a solution with larger duct sizes and consequently lower to medium air velocities. When the pressure limitations are increased to 50Pa, the algorithm starts reducing duct dimensions until the critical path achieves a pressure loss of 50Pa. However, because of the reduction of the duct sizes, the velocities rise (> 4 m/s) and thus the pressure losses increase substantially (see figures 6 and 7). As a result, the maximum allowable pressure drop is already reached after reducing only a few duct diameters, thus limiting the price savings.

On the other hand, if the pressure constraint would be reduced below 30Pa (e.g., 20 pa), then this pressure reduction would correspond to a significant cost increase. Since a duct enlargement (i.e., velocity decrease) now leads to a relatively smaller pressure drop (see Fig. 6 and 7), many more ducts have to be enlarged before the pressure drop in the critical path is less than 20 Pa. Consequently, the ductwork costs will increase significantly.

This example demonstrates the need for a tool that supports the design engineer in informed decision-making to achieve superior air distribution systems with optimal design and performance. The development of the ADND algorithm is a fundamental first step in launching such a tool.

4. Conclusion and future research

In this research, the usability of the ADND optimization algorithm is increased by implementing both circular and rectangular fittings. For every feasible layout, generated with the ADND algorithm, the algorithm can detect automatically the location and type (i.e., bend, reducer, tee, or cross) of every fitting in the air distribution network. The pressure losses due to the fittings are calculated using the duct fitting database of ASHRAE.

The importance of a design algorithm, such as the ADND algorithm, that supports the design engineer in its decision-making, is demonstrated using a test case. It is clear that the design choices (e.g., duct sizes and layout) have a major impact on both the cost and performance of the air distribution network.

Although the ADND algorithm shows promising results, several features can still be added to increase its flexibility and usability in practice, e.g.:

- The extension of the objective function with other objectives, e.g., minimization of the energy costs, maintenance costs, and installation costs.
- The implementation of additional components, e.g., silencers, filters, and diffusers.
- The implementation of CAVs and VAVs, so that optimal demand controlled ventilation systems can be designed and evaluated.
- Models that can evaluate the generated designs in terms of air quality, comfort, and acoustics.
- After all component models have been implemented in the ADND algorithm, a validation on system level has to be conducted.

The implementation of these features in the ADND algorithm is part of future research.

5. Acknowledgement

This work has been supported by the Flemish Agency for Innovation and Entrepreneurship (VLAIO) in the Flux50 project Smart Ventilation (HBC.2020.2520).

6. Appendices

Appendix 1- Input data test case

Start node duct	End node duct	Length (m)	H_{max} (m)	V_{max} (m/s)
1	2	3.2	0.45	5
1	13	2.5	0.5	8
2	3	4.9	0.45	5
2	14	2.5	0.35	5
3	4	3.4	0.45	5
3	15	2.5	0.35	5
4	5	1.1	0.45	5
4	16	2.5	0.35	5
5	6	1.3	0.45	5
5	17	2.5	0.35	5
6	7	2.4	0.4	5
6	18	2.5	0.35	5
7	8	1.3	04	5
7	19	2.5	0.35	5
8	9	1.1	0.4	5
8	20	2.5	0.35	5
9	10	2.3	0.4	5
9	21	2.5	0.35	5
10	11	1.1	0.35	5
10	22	2.5	0.35	5
11	12	1.25	0.35	5
11	23	2.5	0.35	5
12	24	2.5	0.35	5
13	14	3.2	0.5	8
13	25	2.5	0.45	8
14	15	4.9	0.5	5
14	26	2.5	0.45	5
15	16	3.4	0.5	5
15	27	2.5	0.45	5
16	17	1.1	0.45	5
16	28	2.5	0.35	5
17	18	1.3	0.45	5
17	29	2.5	0.35	5
18	19	2.4	0.45	5
18	30	2.5	0.35	5
19	20	1.3	0.45	5
19	31	2.5	0.35	5
20	21	1.1	0.4	5
20	32	2.5	0.35	5
21	22	2.3	0.4	5
21	33	2.5	0.35	5
22	23	1.1	0.4	5
22	34	2.5	0.35	5
23	24	1.25	0.35	5
23	35	2.5	0.35	5
24	36	2.5	0.35	5
25	26	3.2	0.45	5
26	27	4.9	0.45	5
27	28	3.4	0.45	5
28	29	1.1	0.4	5
29	30	1.3	0.4	5
30	31	2.4	0.4	5
31	32	1.3	0.4	5
32	33	1.1	0.4	5
33	34	2.3	0.35	5
34	35	1.1	0.35	5
35	35	1.25	0.35	5
0	13	4	0.5	8

Appendix 2 - Fittings ASHRAE [2]

Component	Component ID	Input parameters
Rectangular bend 90°	ASHRAE CR3-1	Height h, width w, r/w is assumed to be 0.75
Circular bend 90°	ASHRAE CD3-1	Diameter D r/D is assumed to be 1.5
Rectangular reducer	ASHRAE SR4-1	Ratio of inlet area over the outlet area, reduction angle θ
Rectangular to circular reducer	ASHRAE SD4-2	Inlet and outlet diameter, reduction angle θ_2
Circular to circular reducer	ASHRAE SD4-1	Inlet and outlet area, angle of the transition θ (i.e., 15° by default)
Rectangular tee (180° outlets)	ASHRAE SR5-15	Ratio of inlet area over the outlet area, ratio of inlet volumetric flow rate over the outlet flow rate
Rectangular to circular tee (90° and straight outlets)	ASHRAE SR5-11	Ratio of inlet area over the outlet area, ratio of inlet volumetric flow rate over the outlet flow rate
Circular tee (90° and straight outlets)	ASHRAE SD5-9	Ratio of inlet area over the outlet area, ratio of inlet volumetric flow rate over the outlet flow rate
Cross (90° and straight)	ASHRAE SD5-24	Ratio of inlet area over the outlet area, ratio of inlet volumetric flow rate over the outlet flow rate

7. References

[1] Jorens S., Verhaert I., Sörensen K. Design optimization of air distribution systems in non-residential buildings. Elsevier. 2018; 175:48-56.

[2] ASHRAE. ASHRAE Handbook – Fundamentals. Chapter 21: Duct Design, pages 21.1-21.67. 2009.

[3] Asiedu Y., Besant R.W., Gu P. HVAC duct system design using genetic algorithms. HVACR research. 2000; 6: 149-173.

[4] Kim T., Spitler J.D., Delahoussaye R.D. Optimum duct design for variable air volume systems – part 1: problem domain analysis of vav duct systems and part 2: optimization of vav duct systems. ASHRAE Transactions. 2002; 108: 96-127.

[5] Mitchel J.W., Braun J.E. Principles of heating, ventilation and air conditioning in buildings. Wiley. 2012.

[6] Jorens S., Verhaert I., Sörensen K. Design optimization of air distribution systems in nonresidential buildings. Antwerp: University of Antwerp; 2021.

[7] Marcus D.A. Graph theory. A problem oriented approach. United States: Mathematical Association of America.

[8] https://www.lindab.com.

The datasets generated and/or analyzed during the current study are not fully available yet, because they are part of a larger research, which will be published in the near future.